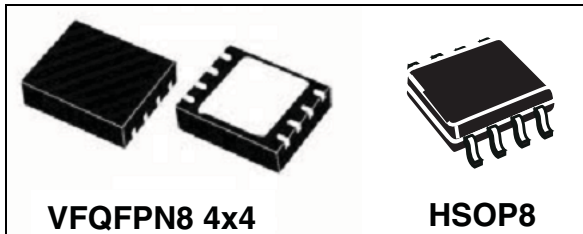


4 A monolithic step-down current source with synchronous rectification

Datasheet - production data



Applications

- High brightness LED driving
- Halogen bulb replacement
- General lighting
- Signage

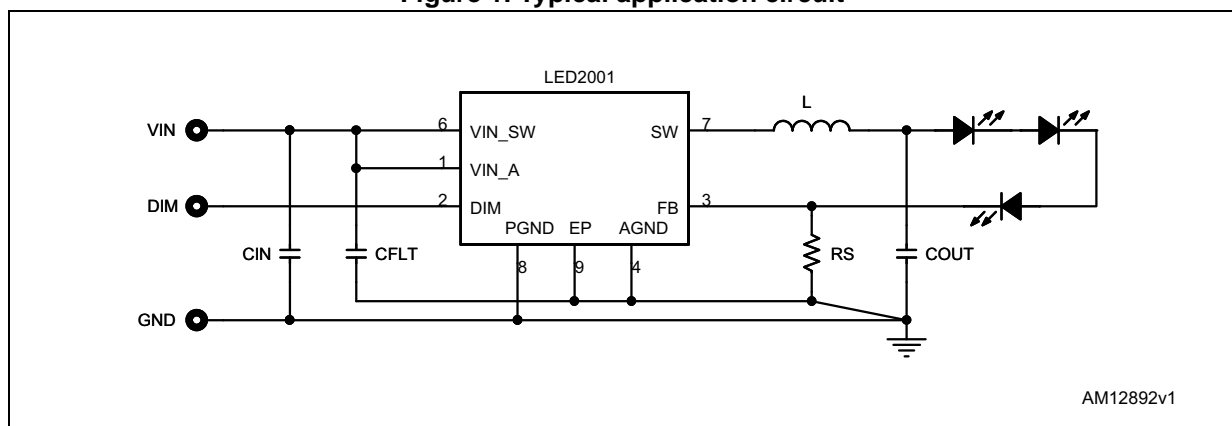
Features

- 3.0 V to 18 V operating input voltage range
- 850 kHz fixed switching frequency
- 100 mV typ. current sense voltage drop
- PWM dimming
- $\pm 7\%$ output current accuracy
- Synchronous rectification
- 95 m Ω HS / 69 m Ω LS typical $R_{DS(on)}$
- Peak current mode architecture
- Embedded compensation network
- Internal current limiting
- Ceramic output capacitor compliant
- Thermal shutdown

Description

The LED2001 is an 850 kHz fixed switching frequency monolithic step-down DC-DC converter designed to operate as precise constant current source with an adjustable current capability up to 4 A DC. The embedded PWM dimming circuitry features LED brightness control. The regulated output current is set connecting a sensing resistor to the feedback pin. The embedded synchronous rectification and the 100 mV typical R_{SENSE} voltage drop enhance the efficiency performance. The size of the overall application is minimized thanks to the high switching frequency and ceramic output capacitor compatibility. The device is fully protected against thermal overheating, overcurrent and output short-circuit. The LED2001 is available in VFQFPN 4 mm x 4 mm 8-lead package, and HSOP8.

Figure 1. Typical application circuit



Contents

| | | |
|----------|---|-----------|
| 1 | Pin settings | 6 |
| 1.1 | Pin connection | 6 |
| 1.2 | Pin description | 6 |
| 2 | Maximum ratings | 7 |
| 3 | Thermal data | 7 |
| 4 | Electrical characteristics | 8 |
| 5 | Functional description | 9 |
| 5.1 | Power supply and voltage reference | 10 |
| 5.2 | Voltage monitor | 10 |
| 5.3 | Soft-start | 10 |
| 5.4 | Error amplifier | 10 |
| 5.5 | Thermal shutdown | 11 |
| 6 | Application notes | 12 |
| 6.1 | Closing the loop | 12 |
| 6.2 | $G_{CO}(s)$ control to output transfer function | 12 |
| 6.3 | Error amplifier compensation network | 13 |
| 6.4 | LED small signal model | 15 |
| 6.5 | Total loop gain | 17 |
| 6.6 | Dimming operation | 18 |
| 6.6.1 | Dimming frequency vs. dimming depth | 20 |
| 6.7 | eDesign studio software | 21 |
| 7 | Application information | 22 |
| 7.1 | Component selection | 22 |
| 7.1.1 | Sensing resistor | 22 |
| 7.1.2 | Inductor and output capacitor selection | 22 |
| 7.1.3 | Input capacitor | 24 |
| 7.2 | Layout considerations | 26 |

| | | |
|-----------|--------------------------------------|-----------|
| 7.3 | Thermal considerations | 27 |
| 7.4 | Short-circuit protection | 28 |
| 7.5 | Application circuit | 30 |
| 8 | Typical characteristics | 34 |
| 9 | Ordering information | 36 |
| 10 | Package mechanical data | 37 |
| 11 | Revision history | 41 |

List of tables

| | | |
|-----------|--|----|
| Table 1. | Pin description | 6 |
| Table 2. | Absolute maximum ratings | 7 |
| Table 3. | Thermal data | 7 |
| Table 4. | Electrical characteristics | 8 |
| Table 5. | Uncompensated error amplifier characteristics. | 11 |
| Table 6. | Inductor selection | 24 |
| Table 7. | List of ceramic capacitors for the LED2001 | 25 |
| Table 8. | Component list | 31 |
| Table 9. | Ordering information | 36 |
| Table 10. | VFQFPN8 (4x4x1.08 mm) mechanical data | 37 |
| Table 11. | HSOP8 mechanical data | 39 |
| Table 12. | Document revision history | 41 |

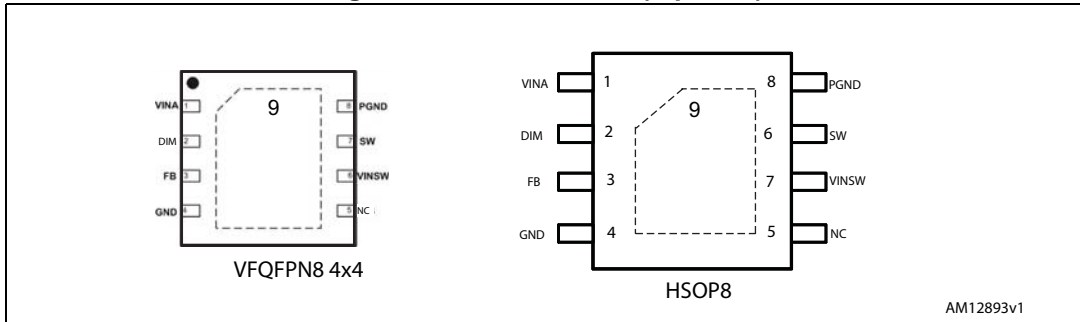
List of figures

| | | |
|------------|--|----|
| Figure 1. | Typical application circuit | 1 |
| Figure 2. | Pin connection (top view) | 6 |
| Figure 3. | LED2001 block diagram | 9 |
| Figure 4. | Internal circuit | 10 |
| Figure 5. | Block diagram of the loop | 12 |
| Figure 6. | Transconductance embedded error amplifier | 14 |
| Figure 7. | Equivalent series resistor | 16 |
| Figure 8. | Load equivalent circuit | 16 |
| Figure 9. | Module plot | 18 |
| Figure 10. | Phase plot. | 18 |
| Figure 11. | Dimming operation example | 19 |
| Figure 12. | LED current falling edge operation | 20 |
| Figure 13. | Dimming signal | 21 |
| Figure 14. | eDesign studio screenshot | 21 |
| Figure 15. | Equivalent circuit. | 23 |
| Figure 16. | Layout example | 26 |
| Figure 17. | Switching losses | 27 |
| Figure 18. | Constant current protection triggering Hiccup mode | 30 |
| Figure 19. | Demonstration board application circuit | 30 |
| Figure 20. | PCB layout (component side) DFN package | 31 |
| Figure 21. | PCB layout (bottom side) DFN package | 32 |
| Figure 22. | PCB layout (component side) HSOP8 package | 32 |
| Figure 23. | PCB layout (bottom side) HSOP8 package | 33 |
| Figure 24. | Soft-start | 34 |
| Figure 25. | Load regulation | 34 |
| Figure 26. | Dimming operation | 34 |
| Figure 27. | LED current rising edge | 34 |
| Figure 28. | LED current falling edge | 34 |
| Figure 29. | Hiccup current protection | 34 |
| Figure 30. | OCP blanking time | 35 |
| Figure 31. | Thermal shutdown protection | 35 |
| Figure 32. | VFQFPN8 (4x4x1.08 mm) package dimensions. | 38 |
| Figure 33. | HSOP8 package dimensions | 40 |

1 Pin settings

1.1 Pin connection

Figure 2. Pin connection (top view)



1.2 Pin description

Table 1. Pin description

| Package/pin | | Type | Description |
|-------------|-------|-------------------|---|
| VFQFPN8 4x4 | HSOP8 | | |
| 1 | 1 | VIN _A | Analog circuitry power supply connection |
| 2 | 2 | DIM | Dimming control input. Logic low prevents the switching activity, logic high enables it. A square wave on this pin implements LED current PWM dimming. Connect to VIN _A if not used (see Section 6.6) |
| 3 | 3 | FB | Feedback input. Connect a proper sensing resistor to set the LED current |
| 4 | 4 | AGND | Analog circuitry ground connection |
| 5 | - | NC | Not connected |
| 6 | 6 | VIN _{SW} | Power input voltage |
| 7 | 7 | SW | Regulator switching pin |
| 8 | 8 | PGND | Power ground |
| ep | ep | Exposed pad | Connect the exposed pad to AGND |

2 Maximum ratings

Table 2. Absolute maximum ratings

| Symbol | Parameter | Value | Unit |
|------------|---|-------------------|------|
| V_{INSW} | Power input voltage | -0.3 to 20 | V |
| V_{INA} | Input voltage | -0.3 to 20 | |
| V_{DIM} | Dimming voltage | -0.3 to V_{INA} | |
| V_{SW} | Output switching voltage | -1 to V_{IN} | |
| V_{PG} | Power Good | -0.3 to V_{IN} | |
| V_{FB} | Feedback voltage | -0.3 to 2.5 | |
| I_{FB} | FB current | -1 to +1 | mA |
| P_{TOT} | Power dissipation at $T_A < 60\text{ °C}$ | 2 | W |
| T_{OP} | Operating junction temperature range | -40 to 150 | °C |
| T_{stg} | Storage temperature range | -55 to 150 | °C |

3 Thermal data

Table 3. Thermal data

| Symbol | Parameter | Value | Unit | |
|------------|--|-------------|------|------|
| R_{thJA} | Maximum thermal resistance junction-ambient ⁽¹⁾ | VFQFPN8 4x4 | 40 | °C/W |
| | | HSOP8 | | |

1. Package mounted on demonstration board.

4 Electrical characteristics

T_J=25 °C, V_{CC}=12 V, unless otherwise specified.

Table 4. Electrical characteristics

| Symbol | Parameter | Test conditions | Value | | | Unit |
|---------------------------|----------------------------------|------------------------------|-------|------|------|------|
| | | | Min. | Typ. | Max. | |
| V _{IN} | Operating input voltage range | (1) | 3 | | 18 | V |
| | Device ON level | | 2.6 | 2.75 | 2.9 | |
| | Device OFF level | | 2.4 | 2.55 | 2.7 | |
| V _{FB} | Feedback voltage | T _J =25 °C | 90 | 97 | 104 | mV |
| | | T _J =125 °C (1) | 90 | 100 | 110 | |
| I _{FB} | V _{FB} pin bias current | (1) | | | 600 | nA |
| R _{DSON-P} | High-side switch on-resistance | I _{SW} =750 mA | | 95 | | mΩ |
| R _{DSON-N} | Low-side switch on-resistance | I _{SW} =750 mA | | 69 | | mΩ |
| I _{LIM} | Maximum limiting current | (2) | | 5.6 | | A |
| Oscillator | | | | | | |
| F _{SW} | Switching frequency | | 0.7 | 0.85 | 1 | MHz |
| D | Duty cycle | (2) | 0 | | 100 | % |
| DC characteristics | | | | | | |
| I _Q | Quiescent current | | | 1.5 | 2.5 | mA |
| Dimming | | | | | | |
| V _{DIM} | DIM threshold voltage | Switching activity | 1.2 | | | V |
| | | Switching activity prevented | | | 0.4 | |
| I _{DIM} | DIM current | | | 2 | | μA |
| Soft-start | | | | | | |
| T _{SS} | Soft-start duration | | | 1 | | ms |
| Protection | | | | | | |
| T _{SHDN} | Thermal shutdown | | | 150 | | °C |
| | Hystereris | | | 15 | | |

1. Specifications referred to T_J from -40 to +125 °C. Specifications in the -40 to +125 °C temperature range are assured by design, characterization and statistical correlation.

2. Guaranteed by design.

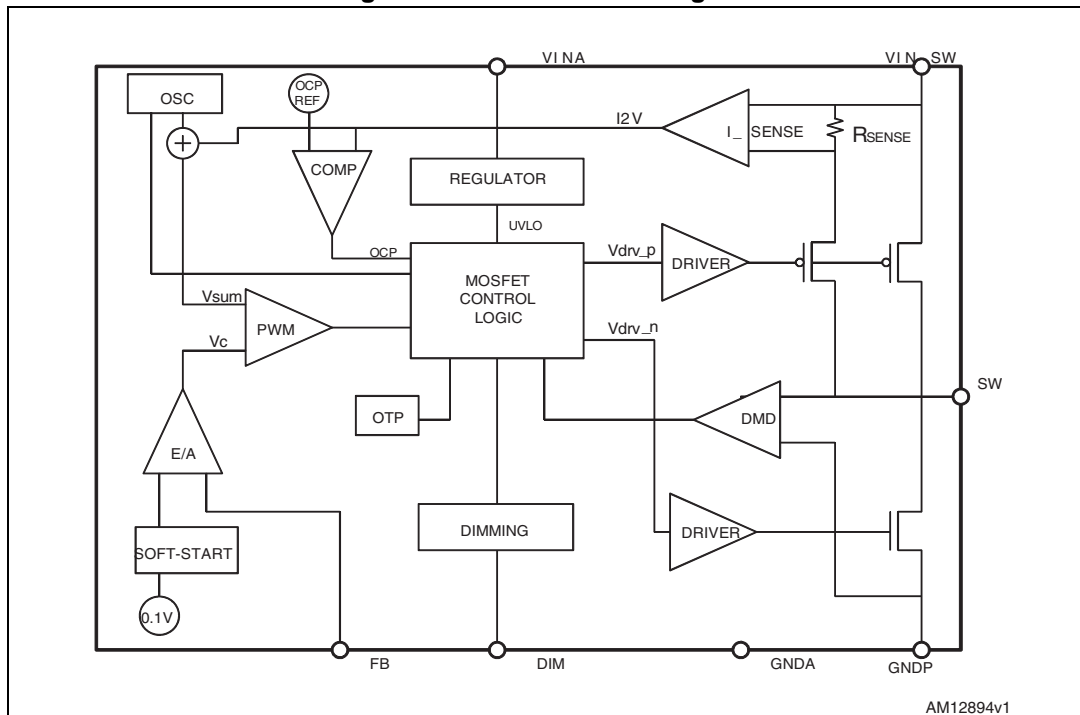
5 Functional description

The LED2001 is based on a “peak current mode” architecture with fixed frequency control. As a consequence, the intersection between the error amplifier output and the sensed inductor current generates the control signal to drive the power switch.

The main internal blocks shown in the block diagram in [Figure 3](#) are:

- high-side and low-side embedded power element for synchronous rectification;
- a fully integrated sawtooth oscillator with a typical frequency of 850 kHz;
- a transconductance error amplifier;
- an high-side current sense amplifier to track the inductor current;
- a pulse width modulator (PWM) comparator and the circuitry necessary to drive the internal power element;
- the soft-start circuitry to decrease the inrush current at power-up;
- the current limitation circuit based on the pulse-by-pulse current protection with frequency divider;
- the dimming circuitry for output current PWM;
- the thermal protection function circuitry.

Figure 3. LED2001 block diagram



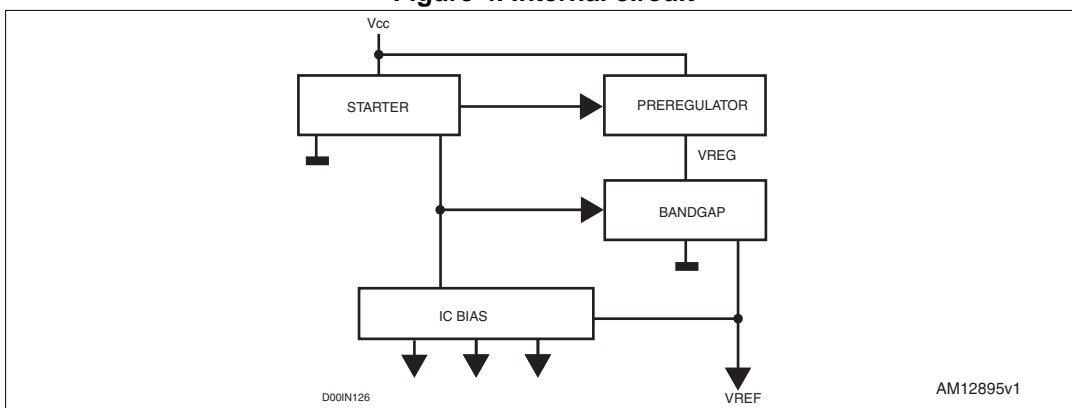
5.1 Power supply and voltage reference

The internal regulator circuit consists of a startup circuit, an internal voltage pre-regulator, the BandGap voltage reference and the bias block that provides current to all the blocks. The starter supplies the startup current to the entire device when the input voltage goes high and the device is enabled. The pre-regulator block supplies the BandGap cell with a pre-regulated voltage that has a very low supply voltage noise sensitivity.

5.2 Voltage monitor

An internal block continuously senses the V_{CC} , V_{ref} and V_{bg} . If the monitored voltages are good, the regulator begins operating. There is also a hysteresis on the V_{CC} (UVLO).

Figure 4. Internal circuit



5.3 Soft-start

The startup phase is implemented ramping the reference of the embedded error amplifier in 1 ms typ. time. It minimizes the inrush current and decreases the stress of the power components at power-up.

During normal operation a new soft-start cycle takes place in case of:

- thermal shutdown event;
- UVLO event.

The soft-start is disabled when DIM input goes high in order to maximize the dimming performance.

5.4 Error amplifier

The voltage error amplifier is the core of the loop regulation. It is a transconductance operational amplifier whose non-inverting input is connected to the internal voltage reference (100 mV), while the inverting input (FB) is connected to the output current sensing resistor.

The error amplifier is internally compensated to minimize the size of the final application.

Table 5. Uncompensated error amplifier characteristics

| Description | Value |
|--------------------|---------------|
| Transconductance | 250 μ S |
| Low frequency gain | 96 dB |
| C_C | 195 pF |
| R_C | 70 K Ω |

The error amplifier output is compared with the inductor current sense information to perform PWM control.

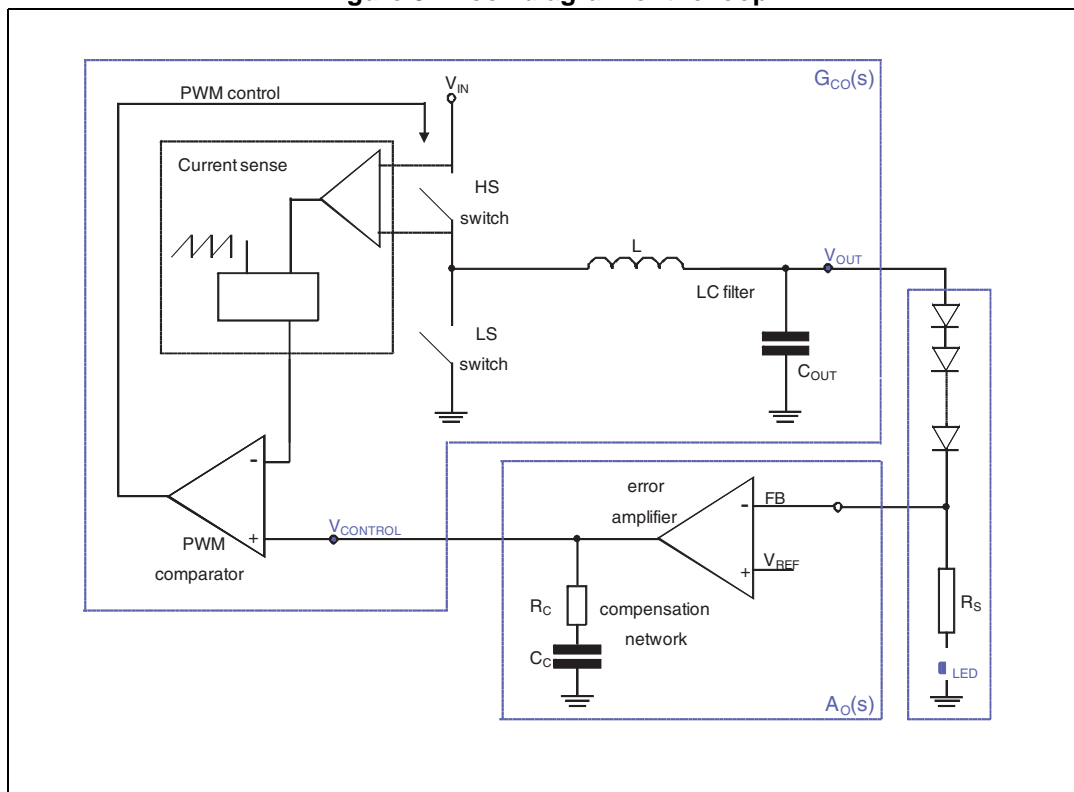
5.5 Thermal shutdown

The shutdown block generates a signal that disables the power stage if the temperature of the chip goes higher than a fixed internal threshold (150 ± 10 °C typical). The sensing element of the chip is close to the PDMOS area, ensuring fast and accurate temperature detection. A 15 °C typical hysteresis prevents the device from turning ON and OFF continuously during the protection operation.

6 Application notes

6.1 Closing the loop

Figure 5. Block diagram of the loop



6.2 $G_{CO}(s)$ control to output transfer function

The accurate control to output transfer function for a buck peak current mode converter can be written as:

Equation 1

$$G_{CO}(s) = \frac{R_0}{R_i} \cdot \frac{1}{1 + \frac{R_0 \cdot T_{SW}}{L} \cdot [m_C \cdot (1 - D) - 0.5]} \cdot \frac{\left(1 + \frac{s}{\omega_z}\right)}{\left(1 + \frac{s}{\omega_p}\right)} \cdot F_H(s)$$

where R_0 represents the load resistance, R_i the equivalent sensing resistor of the current sense circuitry, ω_p the single pole introduced by the LC filter and ω_z the zero given by the ESR of the output capacitor.

$F_H(s)$ accounts for the sampling effect performed by the PWM comparator on the output of the error amplifier that introduces a double pole at one half of the switching frequency.

Equation 2

$$\omega_z = \frac{1}{ESR \cdot C_{OUT}}$$

Equation 3

$$\omega_p = \frac{1}{R_{LOAD} \cdot C_{OUT}} + \frac{m_C \cdot (1-D) - 0.5}{L \cdot C_{OUT} \cdot f_{SW}}$$

where:

Equation 4

$$\begin{cases} m_C = 1 + \frac{S_e}{S_n} \\ S_e = V_{pp} \cdot f_{SW} \\ S_n = \frac{V_{IN} - V_{OUT}}{L} \cdot R_i \end{cases}$$

S_n represents the slope of the sensed inductor current, S_e the slope of the external ramp (V_{pp} peak-to-peak amplitude) that implements the slope compensation to avoid sub-harmonic oscillations at duty cycle over 50%.

The sampling effect contribution $F_H(s)$ is:

Equation 5

$$F_H(s) = \frac{1}{1 + \frac{s}{\omega_n \cdot Q_P} + \frac{s^2}{\omega_n^2}}$$

where:

Equation 6

$$\omega_n = \pi \cdot f_{SW}$$

and

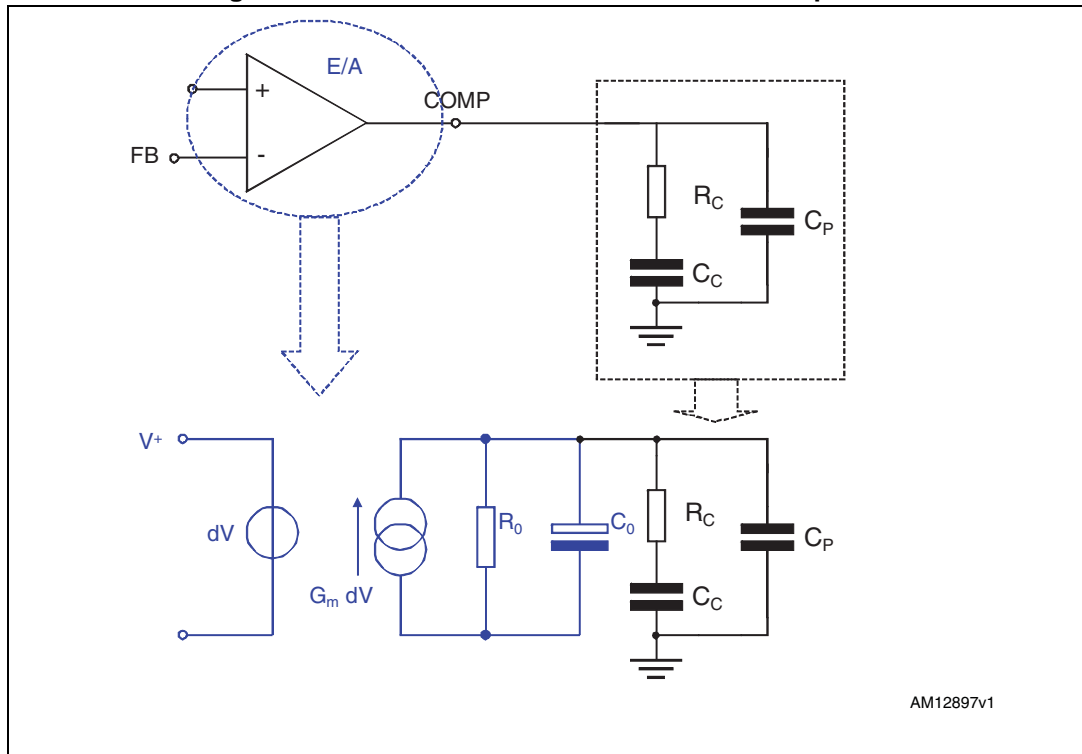
Equation 7

$$Q_P = \frac{1}{\pi \cdot [m_C \cdot (1-D) - 0.5]}$$

6.3 Error amplifier compensation network

The LED2001 embeds (see [Figure 6](#)) the error amplifier and a pre-defined compensation network which is effective in stabilizing the system in most application conditions.

Figure 6. Transconductance embedded error amplifier



R_C and C_C introduce a pole and a zero in the open loop gain. C_P does not significantly affect system stability but it is useful to reduce the noise at the output of the error amplifier.

The transfer function of the error amplifier and its compensation network is:

Equation 8

$$A_0(s) = \frac{A_{V0} \cdot (1 + s \cdot R_C \cdot C_C)}{s^2 \cdot R_0 \cdot (C_0 + C_P) \cdot R_C \cdot C_C + s \cdot (R_0 \cdot C_C + R_0 \cdot (C_0 + C_P) + R_C \cdot C_C) + 1}$$

where $A_{V0} = G_m \cdot R_0$.

The poles of this transfer function are (if $C_C \gg C_0 + C_P$):

Equation 9

$$f_{P\text{LF}} = \frac{1}{2 \cdot \pi \cdot R_0 \cdot C_C}$$

Equation 10

$$f_{P\text{HF}} = \frac{1}{2 \cdot \pi \cdot R_C \cdot (C_0 + C_P)}$$

whereas the zero is defined as:

Equation 11

$$F_Z = \frac{1}{2 \cdot \pi \cdot R_C \cdot C_C}$$

The embedded compensation network is $R_C=70\text{ K}$, $C_C=195\text{ pF}$ while C_P and C_O can be considered as negligible. The error amplifier output resistance is $240\text{ M}\Omega$, so the relevant singularities are:

Equation 12

$$f_z = 11,6\text{ kHz} \quad f_{P_{LF}} = 3,4\text{ Hz}$$

6.4 LED small signal model

Once the system reaches the working condition, the LEDs composing the row are biased and their equivalent circuit can be considered as a resistor for frequencies $\ll 1\text{ MHz}$.

The LED manufacturer typically provides the equivalent dynamic resistance of the LED biased at different DC currents. This parameter is required to study the behavior of the system in the small signal analysis.

For instance, the equivalent dynamic resistance of the Luxeon III Star from Lumiled measured with different biasing current level is reported below:

Equation 13

$$r_{LED} \begin{cases} 1.3\Omega & I_{LED} = 350\text{ mA} \\ 0.9\Omega & I_{LED} = 700\text{ mA} \end{cases}$$

If the LED datasheet does not report the equivalent resistor value, it can be simply derived as the tangent to the diode I-V characteristic in the present working point (see [Figure 7](#)).

Figure 7. Equivalent series resistor

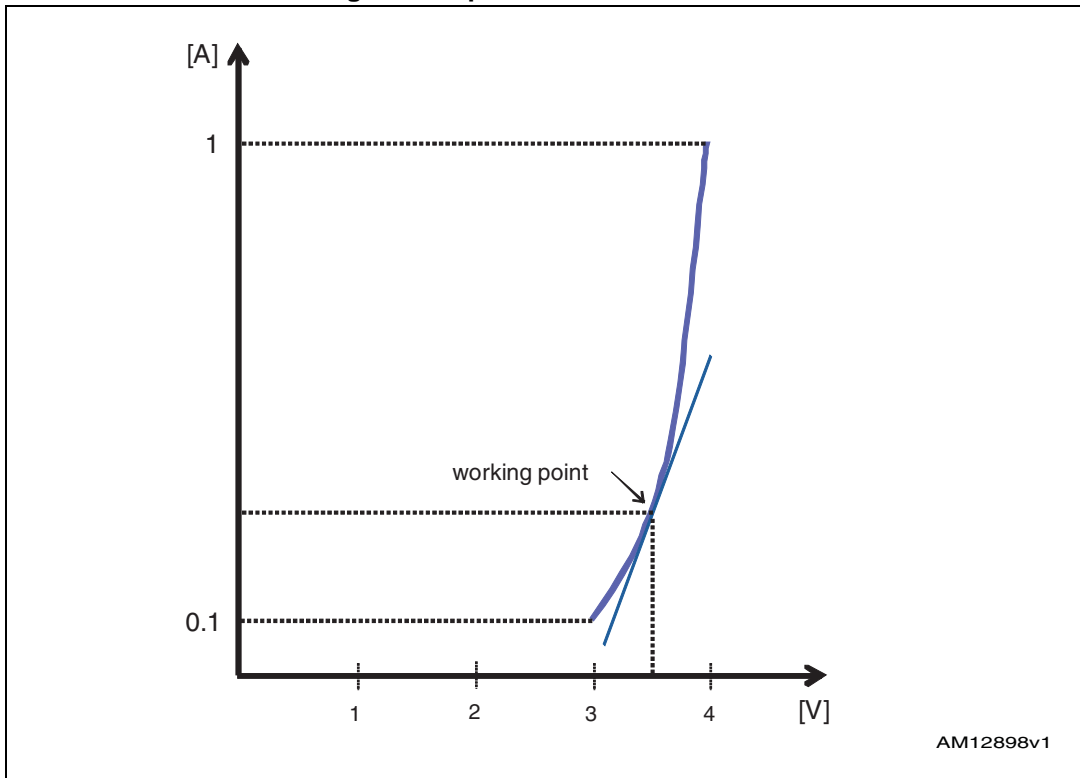
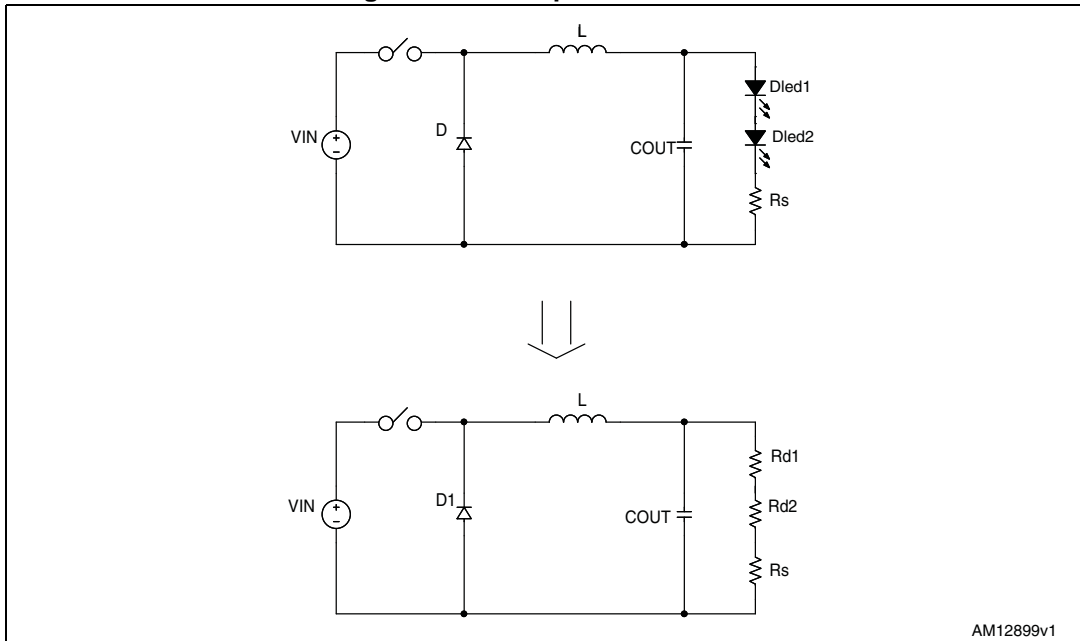


Figure 8 shows the equivalent circuit of the LED constant current generator.

Figure 8. Load equivalent circuit



As a consequence, the LED equivalent circuit gives the $\alpha_{LED}(s)$ term correlating the output voltage with the high impedance FB input:

Equation 14

$$\alpha_{LED}(n_{LED}) = \frac{R_{SENSE}}{n_{LED} \cdot r_{LED} + R_{SENSE}}$$

6.5 Total loop gain

In summary, the open loop gain can be expressed as:

Equation 15

$$G(s) = G_{CO}(s) \cdot A_0(s) \cdot \alpha_{LED}(n_{LED})$$

Example 1

Design specification:

$V_{IN}=12\text{ V}$, $V_{FW_LED}=3.5\text{ V}$, $n_{LED}=2$, $r_{LED}=1.1\ \Omega$, $I_{LED}=4\text{ A}$, $I_{LED\text{ RIPPLE}}=2\%$

The inductor and capacitor value are dimensioned in order to meet the $I_{LED\text{ RIPPLE}}$ specification (see [Section 7.1.2](#) for output capacitor and inductor selection guidelines):

$L=2.2\ \mu\text{H}$, $C_{OUT}=2.2\ \mu\text{F}$ MLCC (negligible ESR)

Accordingly, with [Section 7.1.1](#) the sensing resistor value is:

Equation 16

$$R_S = \frac{100\text{ mV}}{4\text{ A}} \cong 25\text{ m}\Omega$$

Equation 17

$$\alpha_{LED}(n_{LED}) = \frac{R_{SENSE}}{n_{LED} \cdot r_{LED} + R_{SENSE}} = \frac{25\text{ m}\Omega}{2 \cdot 1.1\ \Omega + 25\text{ m}\Omega} = 0.011$$

The gain and phase margin Bode diagrams are plotted respectively in [Figure 9](#) and [Figure 10](#).

Figure 9. Module plot

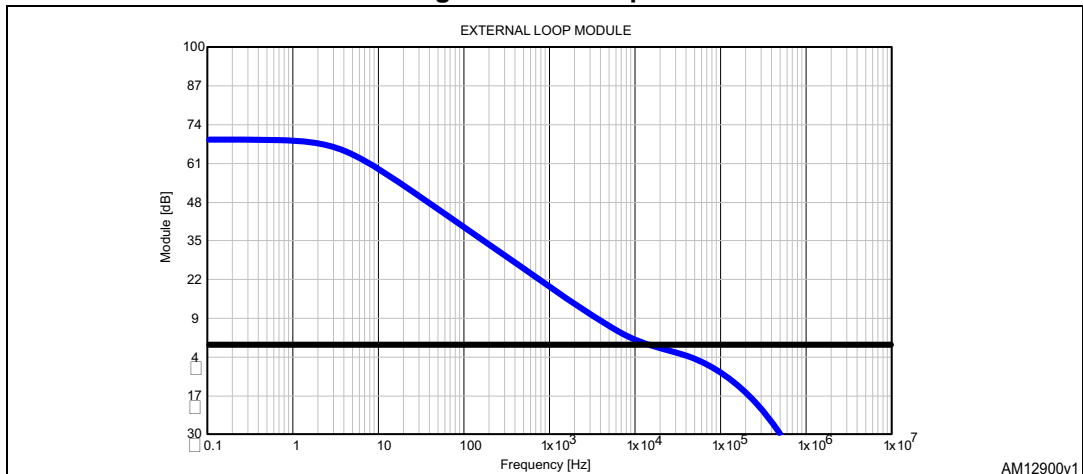
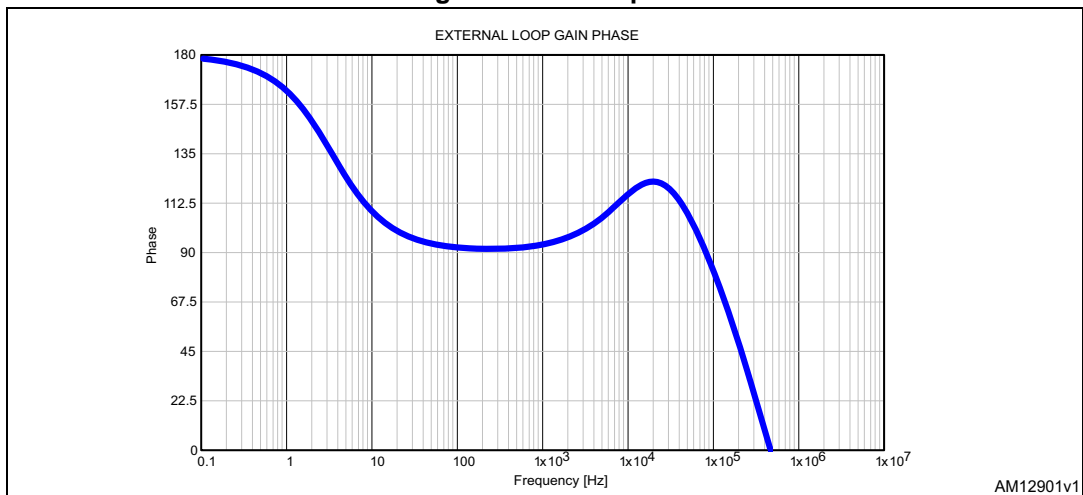


Figure 10. Phase plot



The cut-off frequency and the phase margin are:

Equation 18

$$f_C = 14 \text{ kHz} \quad \text{pm} = 120^\circ$$

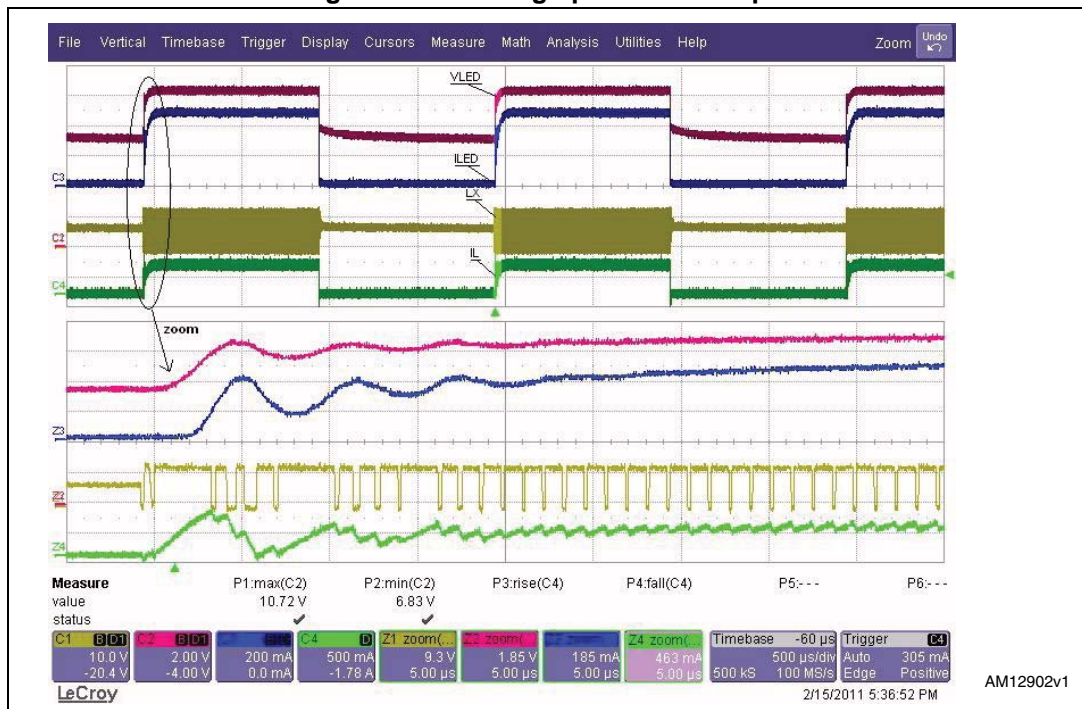
6.6 Dimming operation

The dimming input disables the switching activity, masking the PWM comparator output.

The inductor current dynamic when dimming input goes high depends on the designed system response. The best dimming performance is obtained maximizing the bandwidth and phase margin, when it is possible.

As a general rule, the output capacitor minimization improves the dimming performance.

Figure 11. Dimming operation example



In fact, when dimming enables the switching activity, a small capacitor value is fast charged with low inductor value. As a consequence, the LEDs current rising edge time is improved and the inductor current oscillation reduced. An oversized output capacitor value requires extra current for fast charge so generating certain inductor current oscillations

The switching activity is prevented as soon as the dimming signal goes low. Nevertheless, the LED current drops to zero only when the voltage stored in the output capacitor goes below a minimum voltage determined by the selected LEDs. As a consequence, a big capacitor value makes the LED current falling time worse than a smaller one.

The LED2001 embeds dedicated circuitry to improve LED current falling time.

As soon as the dimming input goes low, the low-side is kept enabled to discharge C_{OUT} until the LED current drops to 60% of the nominal current. A negative current limitation (-1 A typical) protects the device during this operation (see [Figure 12](#)).

Figure 12. LED current falling edge operation



6.6.1 Dimming frequency vs. dimming depth

As seen in [Section 6.6](#), the LEDs current rising and falling edge time mainly depends on the system bandwidth (T_{RISE}) and the selected output capacitor value (T_{RISE} and T_{FALL}).

The dimming performance depends on the minimum current pulse shape specification of the final application. The ideal minimum current pulse has rectangular shape, however, it degenerates into a trapezoid or, at worst, into a triangle, depending on the ratio $(T_{RISE} + T_{FALL}) / T_{DIM}$.

Equation 19

$$\begin{matrix} \text{rectangle} \\ \frac{T_{RISE} + T_{FALL}}{T_{DIM}} \ll 1 \end{matrix} \quad \rightarrow \quad \begin{matrix} \text{trapezoid} \\ \frac{T_{RISE} + T_{FALL}}{T_{DIM}} < 1 \end{matrix} \quad \rightarrow \quad \begin{matrix} \text{triangle} \\ \frac{T_{RISE} + T_{FALL}}{T_{DIM}} = 1 \end{matrix}$$

The small signal response in [Figure 11](#) and [Figure 12](#) is considered as an example.

Equation 20

$$\begin{cases} T_{RISE} \cong 20\mu s \\ T_{FALL} \cong 5\mu s \end{cases}$$

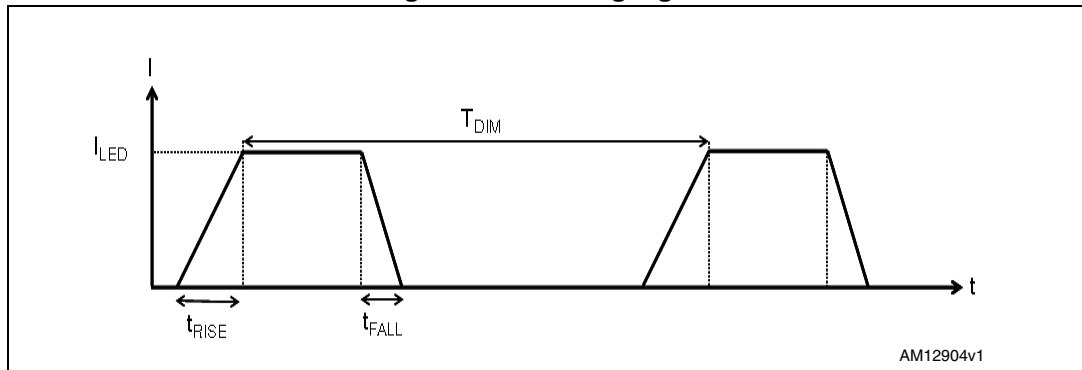
Assuming the minimum current pulse shape specification as:

Equation 21:

$$T_{RISE} + T_{FALL} = 0.5 \cdot T_{MIN_PULSE} = 0.5 \cdot D_{MIN} \cdot T_{DIMMING}$$

it is possible to calculate the maximum dimming depth given the dimming frequency or vice versa.

Figure 13. Dimming signal



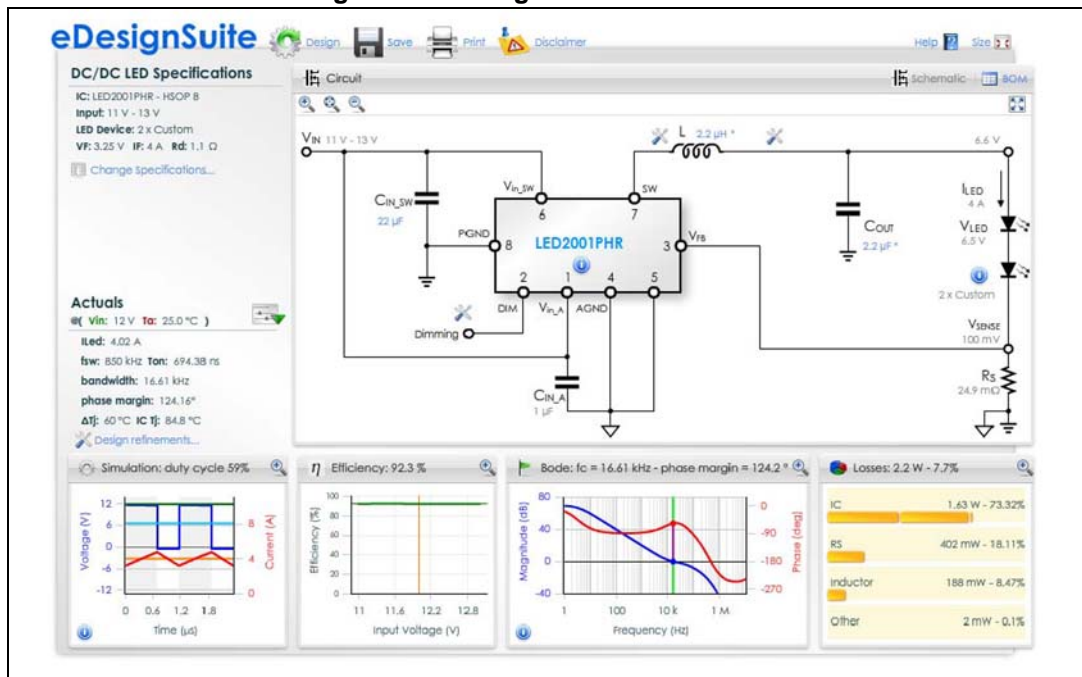
For example, assuming a 1 kHz dimming frequency the maximum dimming depth is 5% or, given a 2% dimming depth, it follows a 200 Hz maximum f_{DIM} .

The LED2001 dimming performance is strictly dependent on the system small signal response. As a consequence, an optimized compensation (good phase margin and bandwidth maximized) and minimized C_{OUT} value are crucial for the best performance.

6.7 eDesign studio software

The LED2001 is supported by the eDesign software which can be viewed online at www.st.com.

Figure 14. eDesign studio screenshot



The software easily supports the component sizing according to the technical information given in this datasheet (see [Section 6](#) and [Section 7](#)).

The end user is requested to fill in the requested information such as the input voltage range, the selected LED parameters and the number of LEDs composing the row.

The software calculates external components according to the internal database. It is also possible to define new components and ask the software to use them.

Bode plots, estimated efficiency and thermal performance are provided.

Finally, the user can save the design and print all the information including the bill of material of the board.

7 Application information

7.1 Component selection

7.1.1 Sensing resistor

In closed loop operation the LED2001 feedback pin voltage is 100 mV, so the sensing resistor calculation is expressed as:

Equation 22

$$R_S = \frac{100 \text{ mV}}{I_{LED}}$$

Since the main loop (see [Section 6.1](#)) regulates the sensing resistor voltage drop, the average current is regulated into the LEDs. The integration period is at minimum $5 \cdot T_{SW}$ since the system bandwidth can be dimensioned up to $f_{SW}/5$ at maximum.

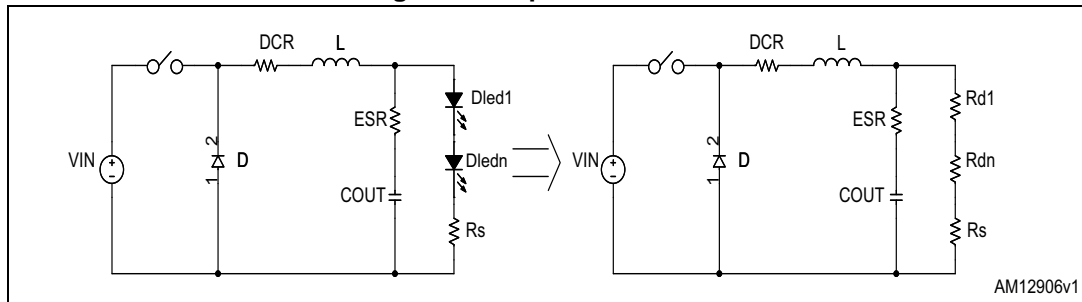
The system performs the output current regulation over a period which is at least five times longer than the switching frequency. The output current regulation neglects the ripple current contribution and its reliance on external parameters like input voltage and output voltage variations (line transient and LED forward voltage spread). This performance can not be achieved with simpler regulation loops such as a hysteretic control.

For the same reason, the switching frequency is constant over the application conditions, which helps to tune the EMI filtering and to guarantee the maximum LED current ripple specification in the application range. This performance can not be achieved using constant ON/OFF-time architecture.

7.1.2 Inductor and output capacitor selection

The output capacitor filters the inductor current ripple that, given the application condition, depends on the inductor value. As a consequence, the LED current ripple, that is the main specification for a switching current source, depends on the inductor and output capacitor selection.

Figure 15. Equivalent circuit



The LED ripple current can be calculated as the inductor ripple current ratio flowing into the output impedance using the Laplace transform (see [Figure 11](#)):

Equation 23

$$\Delta I_{\text{RIPPLE}}(s) = \frac{\frac{8}{\pi^2} \cdot \Delta I_L \cdot (1 + s \cdot \text{ESR} \cdot C_{\text{OUT}})}{1 + s \cdot (R_S + \text{ESR} + n_{\text{LED}} \cdot R_{\text{LED}}) \cdot C_{\text{OUT}}}$$

where the term $\frac{8}{\pi^2}$ represents the main harmonic of the inductor current ripple (which has a triangular shape) and ΔI_L is the inductor current ripple.

Equation 24

$$\Delta I_L = \frac{V_{\text{OUT}}}{L} \cdot T_{\text{OFF}} = \frac{n_{\text{LED}} \cdot V_{\text{FW_LED}} + 100\text{mV}}{L} \cdot T_{\text{OFF}}$$

so L value can be calculated as:

Equation 25

$$L = \frac{n_{\text{LED}} \cdot V_{\text{FW_LED}} + 100\text{mV}}{\Delta I_L} \cdot T_{\text{OFF}} = \frac{n_{\text{LED}} \cdot V_{\text{FW_LED}} + 100\text{mV}}{\Delta I_L} \cdot \left(1 - \frac{n_{\text{LED}} \cdot V_{\text{FW_LED}} + 100\text{mV}}{V_{\text{IN}}}\right)$$

where T_{OFF} is the OFF-time of the embedded high switch, given by $1-D$.

As a consequence, the lower the inductor value (so the higher the current ripple), the higher the C_{OUT} value would be to meet the specification.

A general rule to dimension L value is:

Equation 26

$$\frac{\Delta I_L}{I_{\text{LED}}} \leq 0.5$$

Finally, the required output capacitor value can be calculated equalizing the LED current ripple specification with the module of the Fourier transformer (see [Equation 23](#)) calculated at f_{SW} frequency.

Equation 27

$$|\Delta I_{\text{RIPPLE}}(s=j \cdot \omega)| = \Delta I_{\text{RIPPLE_SPEC}}$$

Example (see [Section Example 1](#)):

$V_{\text{IN}}=12 \text{ V}$, $I_{\text{LED}}=700 \text{ mA}$, $\Delta I_{\text{LED}}/I_{\text{LED}}=2\%$, $V_{\text{FW_LED}}=3.5 \text{ V}$, $\eta_{\text{LED}}=2$.

A lower inductor value maximizes the inductor current slew rate for better dimming performance. [Equation 26](#) becomes:

Equation 28

$$\frac{\Delta I_L}{I_{\text{LED}}} = 0.5$$

which is satisfied selecting a $10 \mu\text{H}$ inductor value.

The output capacitor value must be dimensioned according to [Equation 27](#).

Finally, given the selected inductor value, a $2.2 \mu\text{F}$ ceramic capacitor value keeps the LED current ripple ratio lower than the 2% of the nominal current. An output ceramic capacitor type (negligible ESR) is suggested to minimize the ripple contribution given a fixed capacitor value.

Table 6. Inductor selection

| Manufacturer | Series | Inductor value (μH) | Saturation current (A) |
|------------------|-------------|----------------------------------|------------------------|
| Würth Elektronik | WE-HCI 7040 | 1 to 4.7 | 20 to 7 |
| | WE-HCI 7050 | 4.9 to 10 | 20 to 4.0 |
| Coilcraft | XPL 7030 | 2.2 to 10 | 29 to 7.2 |

7.1.3 Input capacitor

The input capacitor must be able to support the maximum input operating voltage and the maximum RMS input current.

Since step-down converters draw current from the input in pulses, the input current is squared and the height of each pulse is equal to the output current. The input capacitor must absorb all this switching current, whose RMS value can be up to the load current divided by two (worst case, with duty cycle of 50%). For this reason, the quality of these capacitors must be very high to minimize the power dissipation generated by the internal ESR, thereby improving system reliability and efficiency. The critical parameter is usually the RMS current rating, which must be higher than the RMS current flowing through the capacitor. The maximum RMS input current (flowing through the input capacitor) is:

Equation 29

$$I_{\text{RMS}} = I_O \cdot \sqrt{D - \frac{2 \cdot D^2}{\eta} + \frac{D^2}{\eta^2}}$$

where η is the expected system efficiency, D is the duty cycle and I_O is the output DC current. Considering $\eta = 1$ this function reaches its maximum value at $D = 0.5$ and the

equivalent RMS current is equal to I_O divided by 2. The maximum and minimum duty cycles are:

Equation 30

$$D_{MAX} = \frac{V_{OUT} + V_F}{V_{INMIN} - V_{SW}}$$

and

Equation 31

$$D_{MIN} = \frac{V_{OUT} + V_F}{V_{INMAX} - V_{SW}}$$

where V_F is the free-wheeling diode forward voltage and V_{SW} the voltage drop across the internal PDMOS. Considering the range D_{MIN} to D_{MAX} , it is possible to determine the max. I_{RMS} going through the input capacitor. Capacitors that can be considered are:

- Electrolytic capacitors:

these are widely used due to their low price and their availability in a wide range of RMS current ratings.

The only drawback is that, considering ripple current rating requirements, they are physically larger than other capacitors.

- Ceramic capacitors:

if available for the required value and voltage rating, these capacitors usually have a higher RMS current rating for a given physical dimension (due to very low ESR).

The drawback is the considerably high cost.

- Tantalum capacitors:

small tantalum capacitors with very low ESR are becoming more widely available. However, they can occasionally burn if subjected to very high current during charge.

Therefore, it is suggested to avoid this type of capacitor for the input filter of the device as they may be stressed by a high surge current when connected to the power supply.

Table 7. List of ceramic capacitors for the LED2001

| Manufacturer | Series | Capacitor value (μC) | Rated voltage (V) |
|--------------|---------------------|-----------------------------------|-------------------|
| Taiyo yuden | UMK325BJ106MM-T | 10 | 50 |
| Murata | GRM42-2 X7R 475K 50 | 4.7 | 50 |

If the selected capacitor is ceramic (so neglecting the ESR contribution), the input voltage ripple can be calculated as:

Equation 32

$$V_{INPP} = \frac{I_O}{C_{IN} \cdot f_{SW}} \cdot \left[\left(1 - \frac{D}{\eta}\right) \cdot D + \frac{D}{\eta} \cdot (1 - D) \right]$$

7.2 Layout considerations

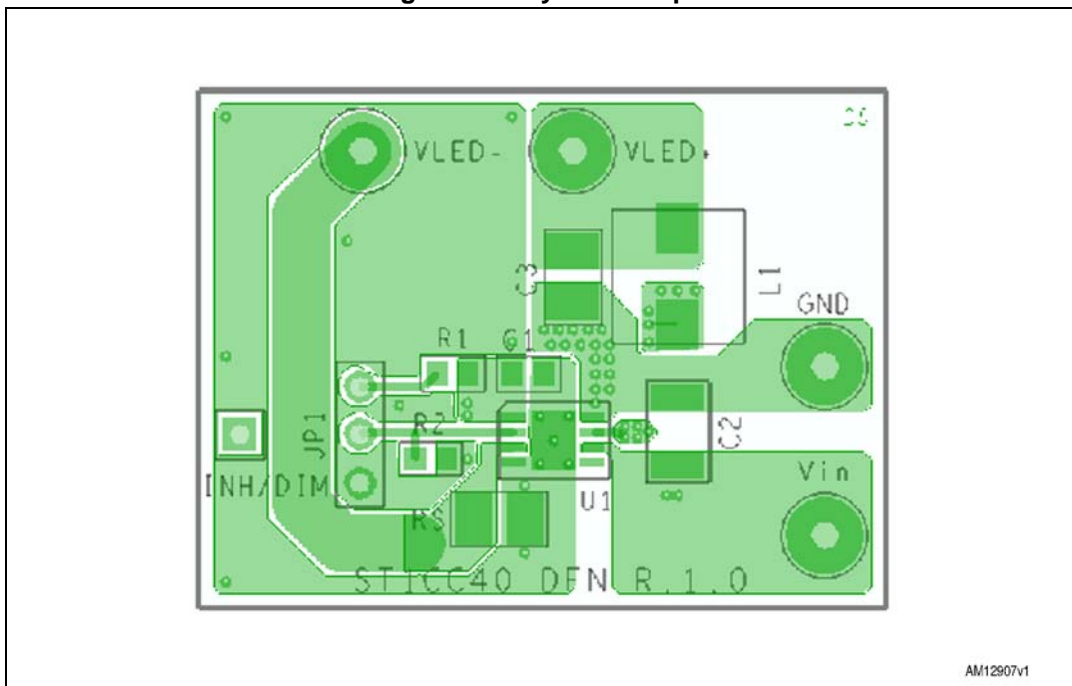
The layout of switching DC-DC converters is very important to minimize noise and interference. Power-generating portions of the layout are the main cause of noise and so high switching current loop areas should be kept as small as possible and lead lengths as short as possible.

High impedance paths (in particular the feedback connections) are susceptible to interference, so they should be as far as possible from the high current paths. A layout example is provided in [Figure 16](#).

The input and output loops are minimized to avoid radiation and high frequency resonance problems. The feedback pin to the sensing resistor path must be designed as short as possible to avoid pick-up noise. Another important issue is the ground plane of the board. As the package has an exposed pad, it is very important to connect it to an extended ground plane in order to reduce the thermal resistance junction-to-ambient.

To increase the design noise immunity, different signal and power ground should be implemented in the layout (see [Section 7.5: Application circuit](#)). The signal ground serves the small signal components, the device analog ground pin, the exposed pad and a small filtering capacitor connected to the VCC pin. The power ground serves the device ground pin and the input filter. The different grounds are connected underneath the output capacitor. Neglecting the current ripple contribution, the current flowing through this component is constant during the switching activity and so this is the cleanest ground point of the buck application circuit.

Figure 16. Layout example



7.3 Thermal considerations

The dissipated power of the device is tied to three different sources:

- Conduction losses due to the R_{DSON} , which are equal to:

Equation 33

$$P_{ON} = R_{DSON_HS} \cdot (I_{OUT})^2 \cdot D$$

$$P_{OFF} = R_{DSON_LS} \cdot (I_{OUT})^2 \cdot (1 - D)$$

where D is the duty cycle of the application. Note that the duty cycle is theoretically given by the ratio between V_{OUT} ($n_{LED} \cdot V_{LED} + 100 \text{ mV}$) and V_{IN} , but in practice it is substantially higher than this value to compensate for the losses in the overall application. For this reason, the conduction losses related to the R_{DSON} increase compared to an ideal case.

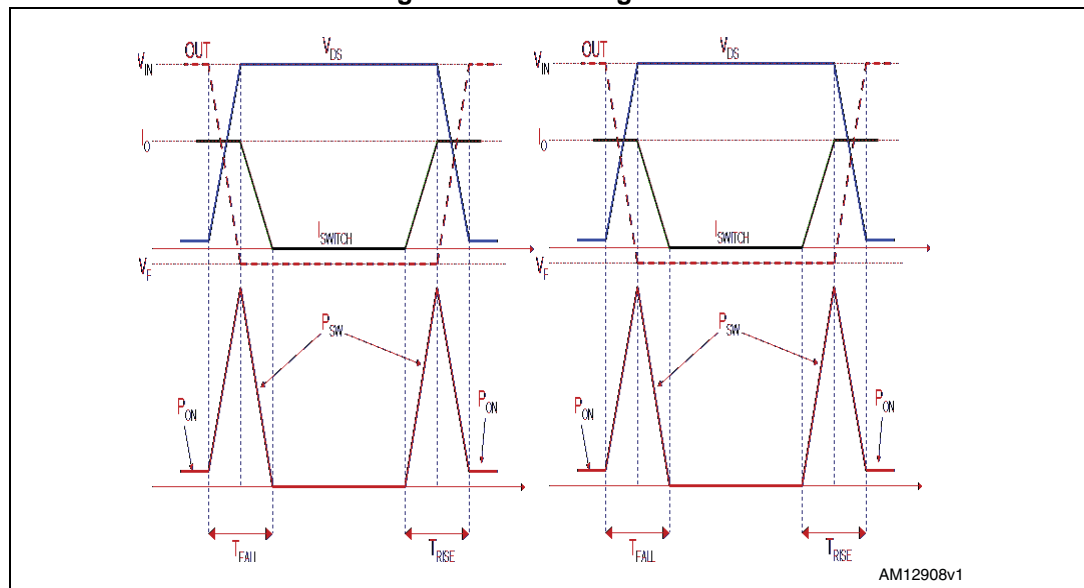
- Switching losses due to turn-ON and turn-OFF. These are derived using the following equation:

Equation 34

$$P_{SW} = V_{IN} \cdot I_{OUT} \cdot \frac{(T_{RISE} + T_{FALL})}{2} \cdot F_{SW} = V_{IN} \cdot I_{OUT} \cdot T_{SW_EQ} \cdot F_{SW}$$

where T_{RISE} and T_{FALL} represent the switching times of the power element that cause the switching losses when driving an inductive load (see [Figure 17](#)). T_{SW} is the equivalent switching time.

Figure 17. Switching losses



- Quiescent current losses.

Equation 35

$$P_Q = V_{IN} \cdot I_Q$$

Example (see [Section Example 1](#)):

$V_{IN}=12\text{ V}$, $V_{FW_LED}=3.5\text{ V}$, $n_{LED}=2$, $I_{LED}=700\text{ mA}$

The typical output voltage is:

Equation 36

$$V_{OUT} = n_{LED} \cdot V_{FW_LED} + V_{FB} = 7.1\text{V}$$

R_{DSON_HS} has a typical value of $95\text{ m}\Omega$ and R_{DSON_LS} is $69\text{ m}\Omega @ 25\text{ }^\circ\text{C}$.

For the calculation we can estimate $R_{DSON_HS} = 140\text{ m}\Omega$ and $R_{DSON_LS} = 100\text{ m}\Omega$ as a consequence of T_j increase during the operation.

T_{SW_EQ} is approximately 12 ns .

I_Q has a typical value of $1.5\text{ mA} @ V_{IN} = 12\text{ V}$.

The overall losses are:

Equation 37

$$P_{TOT} = R_{DSON_HS} \cdot (I_{OUT})^2 \cdot D + R_{DSON_LS} \cdot (I_{OUT})^2 \cdot (1 - D) + V_{IN} \cdot I_{OUT} \cdot f_{SW} \cdot T_{SW} + V_{IN} \cdot I_Q$$

Equation 38

$$P_{TOT} = 0.14 \cdot 0.7^2 \cdot 0.6 + 0.1 \cdot 0.7^2 \cdot 0.4 + 12 \cdot 0.7 \cdot 12 \cdot 10^{-9} \cdot 850 \cdot 10^3 + 12 \cdot 1.5 \cdot 10^{-3} \cong 205\text{mW}$$

The junction temperature of the device is:

Equation 39

$$T_J = T_A + R_{th_{J-A}} \cdot P_{TOT}$$

where T_A is the ambient temperature and $R_{th_{J-A}}$ is the thermal resistance junction-to-ambient. The junction-to-ambient ($R_{th_{J-A}}$) thermal resistance of the device assembled in the HSO8 package and mounted on the board is about $40\text{ }^\circ\text{C/W}$.

Assuming the ambient temperature is around $40\text{ }^\circ\text{C}$, the estimated junction temperature is:

$$T_J = 60 + 0.205 \cdot 40 \cong 68\text{ }^\circ\text{C}$$

7.4 Short-circuit protection

In overcurrent protection mode, when the peak current reaches the current limit threshold, the device disables the power element and it is able to reduce the conduction time down to the minimum value (approximately 100 nsec typical) to keep the inductor current limited. This is the pulse-by-pulse current limitation to implement the constant current protection feature.

In overcurrent condition, the duty cycle is strongly reduced and, in most applications, this is enough to limit the switch current to the current threshold.

The inductor current ripple during ON and OFF phases can be written as:

- ON phase

Equation 40

$$\Delta I_{L\text{ TON}} = \frac{V_{\text{IN}} - V_{\text{OUT}} - (\text{DCR}_L + R_{\text{DSON HS}}) \cdot I}{L} (T_{\text{ON}})$$

- OFF phase

Equation 41

$$\Delta I_{L\text{ TOFF}} = \frac{-(V_{\text{OUT}} + (\text{DCR}_L + R_{\text{DSON LS}}) \cdot I)}{L} (T_{\text{OFF}})$$

where DCR_L is the series resistance of the inductor.

The pulse-by-pulse current limitation is effective to implement constant current protection when:

Equation 42

$$|\Delta I_{L\text{ TON}}| = |\Delta I_{L\text{ TOFF}}|$$

From [Equation 40](#) and [Equation 41](#) it can be seen that the implementation of the constant current protection becomes more critical the lower the V_{OUT} and the higher the V_{IN} .

In fact, in short-circuit condition the voltage applied to the inductor during the OFF-time becomes equal to the voltage drop across parasitic components (typically the DCR of the inductor and the R_{DSON} of the low-side switch) since V_{OUT} is negligible, while during T_{ON} the voltage applied at the inductor is maximized and is approximately equal to V_{IN} .

In general, the worst case scenario is heavy short-circuit at the output with maximum input voltage. [Equation 40](#) and [Equation 41](#) in overcurrent conditions can be simplified to:

Equation 43

$$\Delta I_{L\text{ TON}} = \frac{V_{\text{IN}} - (\text{DCR}_L + R_{\text{DSON HS}}) \cdot I}{L} (T_{\text{ON MIN}}) \cong \frac{V_{\text{IN}}}{L} (90\text{ns})$$

considering T_{ON} which has already been reduced to its minimum.

Equation 44

$$\Delta I_{L\text{ TOFF}} = \frac{-(\text{DCR}_L + R_{\text{DSON LS}}) \cdot I}{L} (T_{\text{SW}} - 90\text{ns}) \cong \frac{-(\text{DCR}_L + R_{\text{DSON LS}}) \cdot I}{L} (1.18\mu\text{s})$$

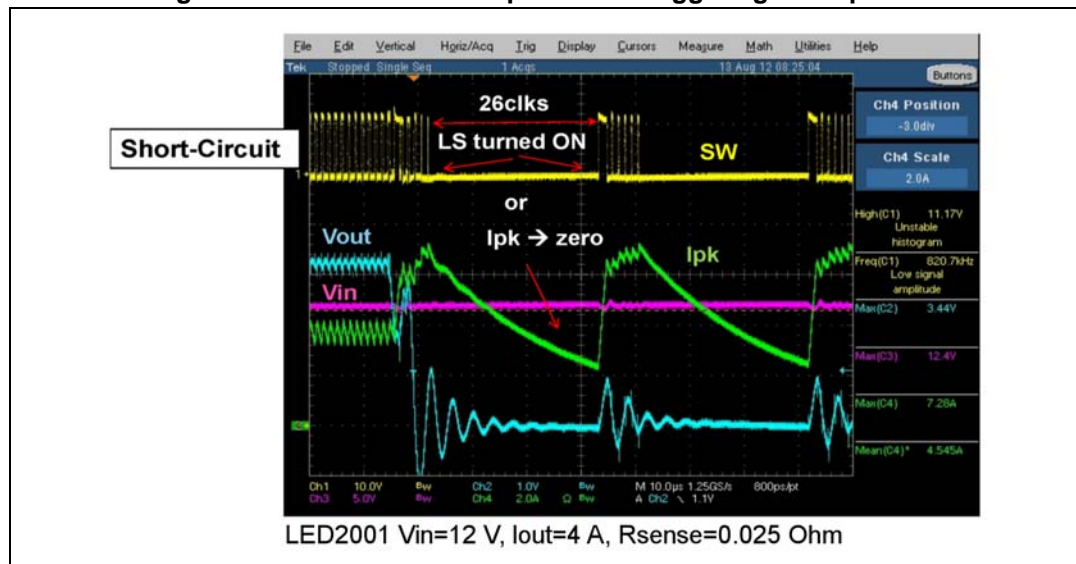
where $T_{\text{SW}} = 1/f_{\text{SW}}$ and considering the nominal f_{SW} .

At higher input voltage $\Delta I_{L\text{ TON}}$ may be higher than $\Delta I_{L\text{ TOFF}}$ and so the inductor current can escalate. As a consequence, the system typically meets [Equation 42](#) at a current level higher than the nominal value thanks to the increased voltage drop across stray components. In most of the application conditions the pulse-by-pulse current limitation is effective to limit the inductor current. Whenever the current escalates, a second level current protection called “Hiccup mode” is enabled. Hiccup protection offers an additional protection against heavy short-circuit conditions at very high input voltage even considering the spread

of the minimum conduction time of the power element. If the hiccup current level (6.2 A typical) is triggered, the switching activity is prevented for 12 cycles.

Figure 18 shows the operation of the constant current protection when a short-circuit is applied at the output at the maximum input voltage.

Figure 18. Constant current protection triggering Hiccup mode



During pulse skipping, high side OFF, low side keeps ON till 26clks finish (13clks for LED2001) or Ipk decreases to be zero value.

7.5 Application circuit

Figure 19. Demonstration board application circuit

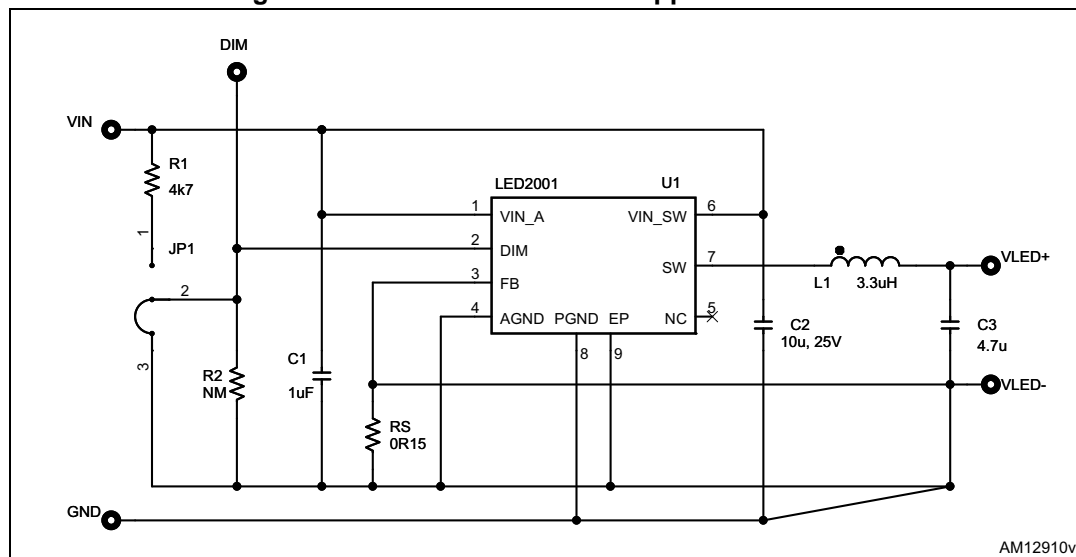


Table 8. Component list

| Reference | Part number | Description | Manufacturer |
|-----------|--------------------|---|--------------|
| C1 | | 1 μ F 25 V (size 0805) | |
| C2 | GRM31CR61E226KE15L | 22 μ F 25 V (size 1206) | Murata |
| C3 | GRM21BR71E475KA73L | 4.7 μ F 25 V (size 0805) | Murata |
| R1 | | 4.7 K Ω 5% (size 0603) | |
| R2 | | Not mounted | |
| Rs | ERJ14BSFR15U | 0.15 Ω 1% (size 1206) | Panasonic |
| L1 | XAL6030-332MEB | 3.3 μ H $I_{SAT} = 8.4$ A (20% drop) $I_{RMS} = 7.3$ A (40 $^{\circ}$ C rise) (size 6.36 x 6.56 x 6.1 mm) | Coilcraft |

Figure 20. PCB layout (component side) DFN package

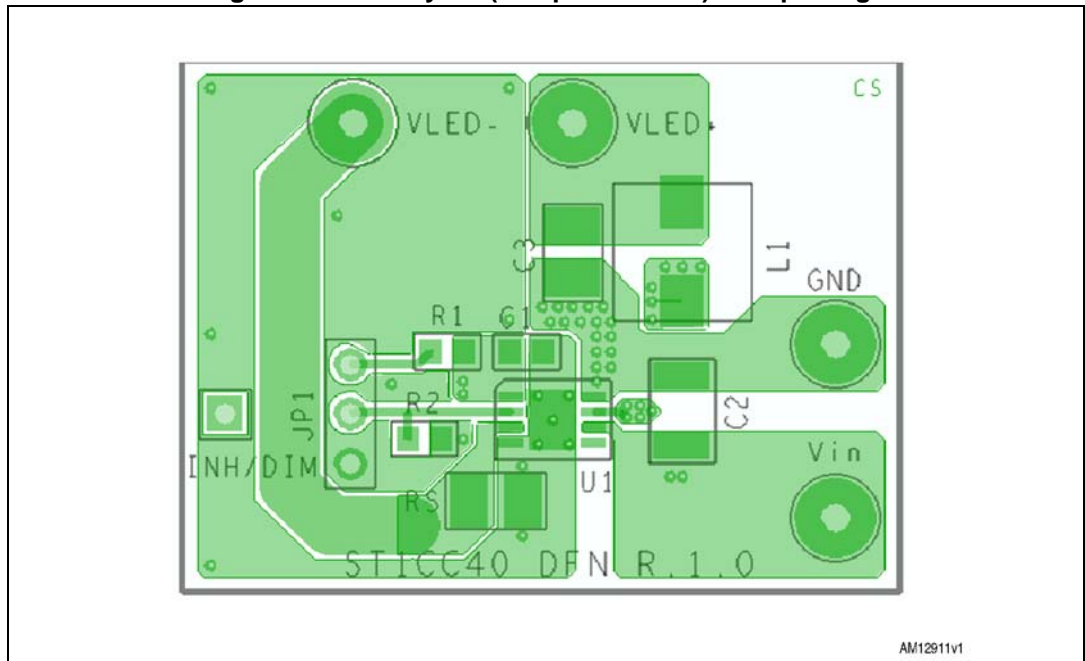
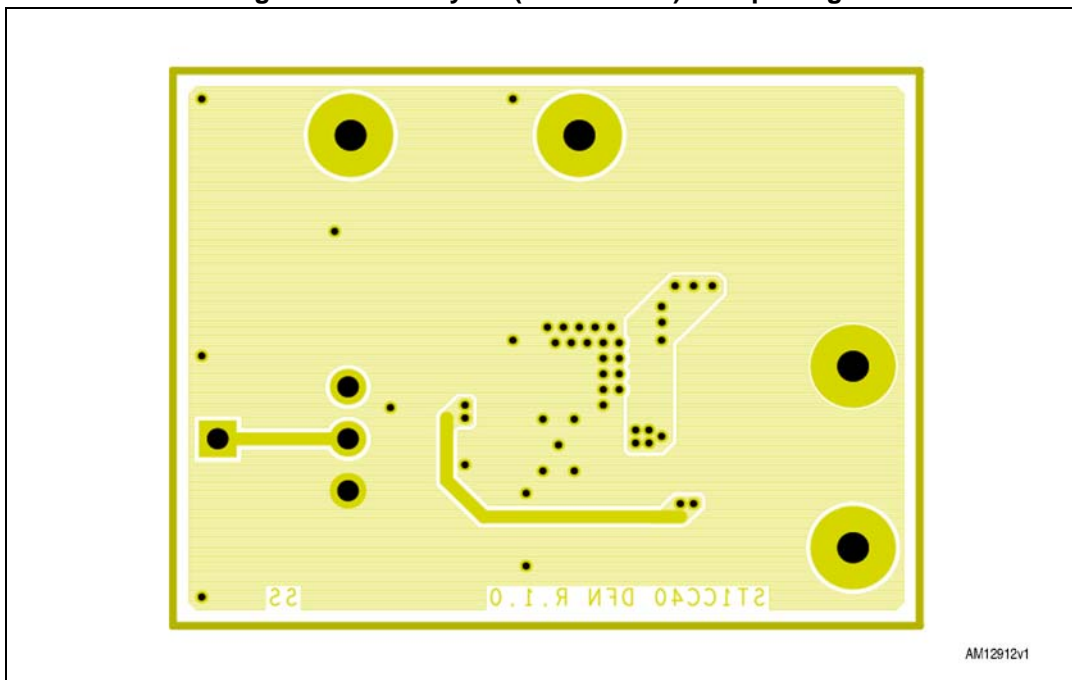
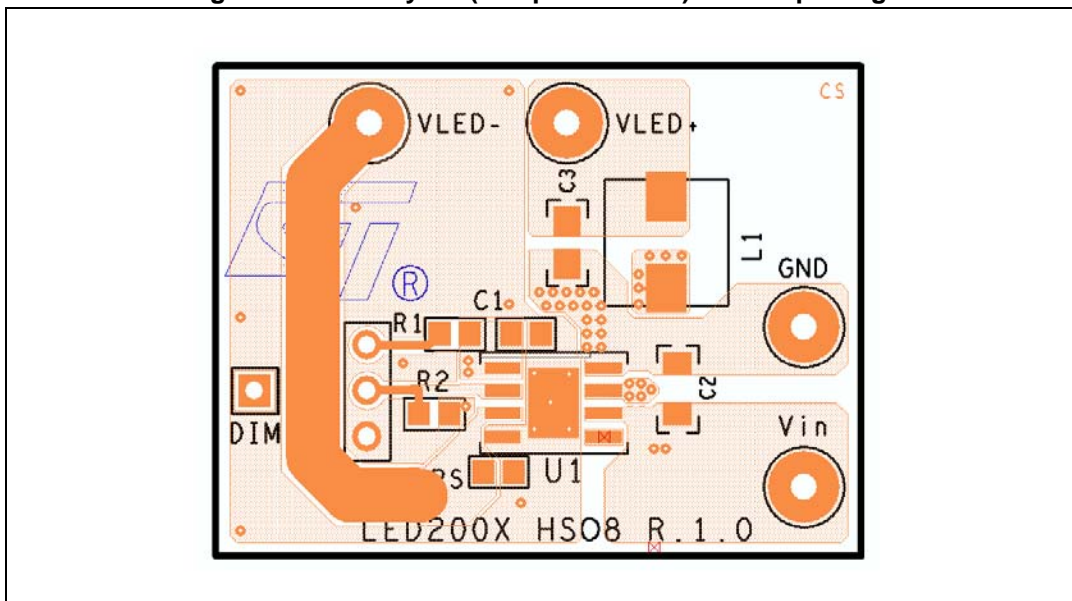


Figure 21. PCB layout (bottom side) DFN package



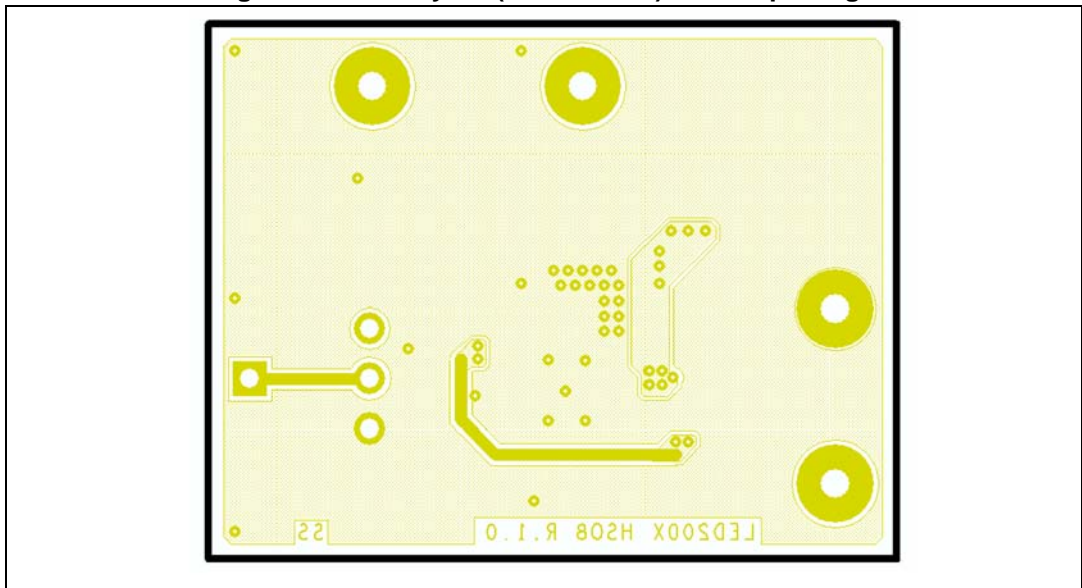
AM12912v1

Figure 22. PCB layout (component side) HSOP8 package



It is strongly recommended that the input capacitors are to be put as close as possible to the pins, see C1 and C2.

Figure 23. PCB layout (bottom side) HSOP8 package



8 Typical characteristics

Figure 24. Soft-start

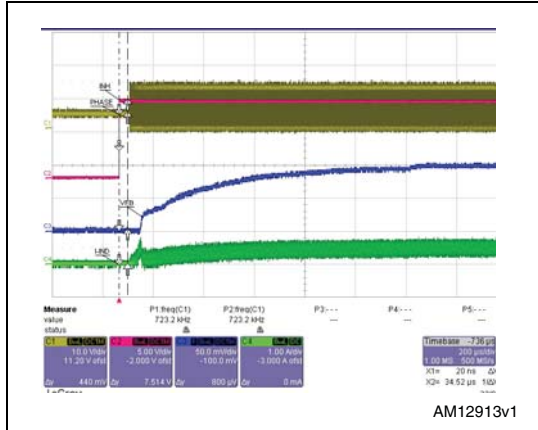


Figure 25. Load regulation

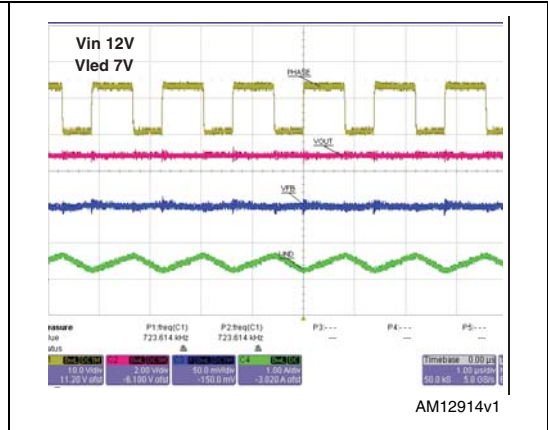


Figure 26. Dimming operation

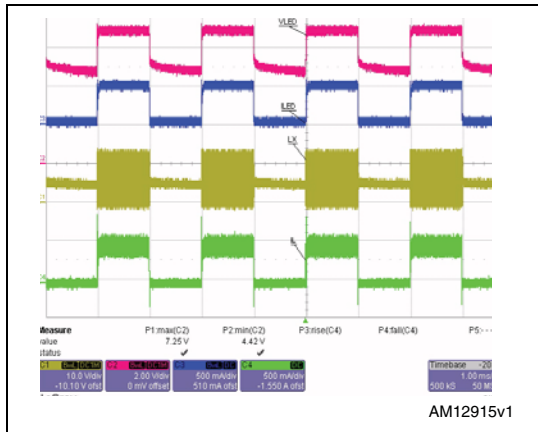


Figure 27. LED current rising edge

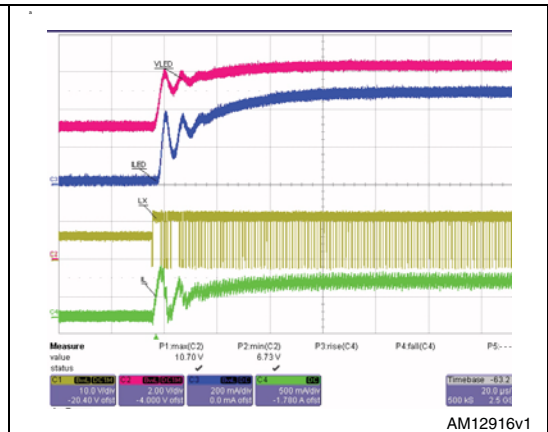


Figure 28. LED current falling edge

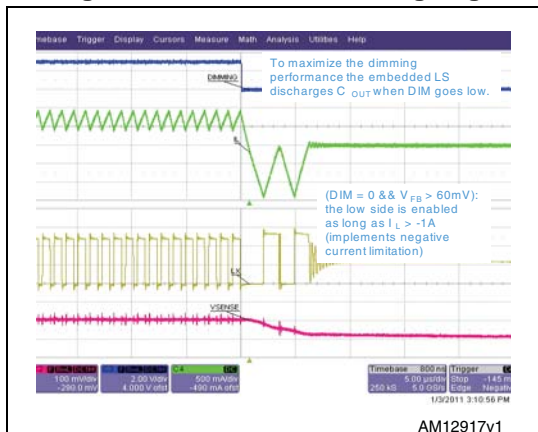


Figure 29. Hiccup current protection

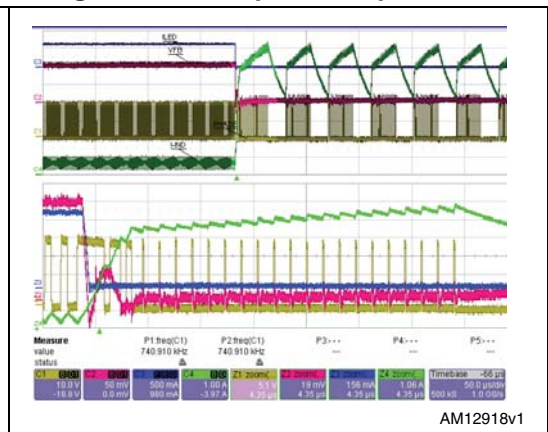


Figure 30. OCP blanking time

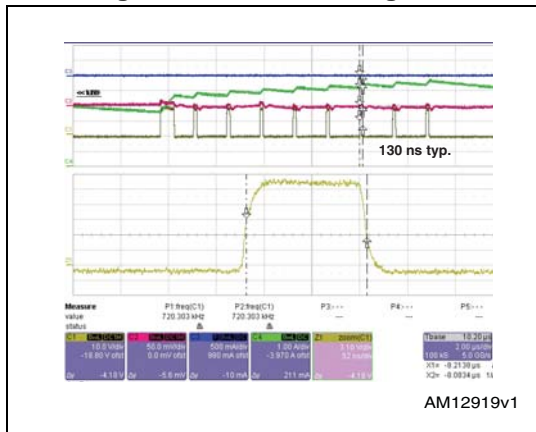


Figure 31. Thermal shutdown protection



9 Ordering information

Table 9. Ordering information

| Order code | Package | Packaging |
|------------|---------------|---------------|
| LED2001PUR | VFQFPN 4x4 8L | Tape and reel |
| LED2001PHR | HSOP8 | |

10 Package mechanical data

In order to meet environmental requirements, ST offers these devices in different grades of ECOPACK[®] packages, depending on their level of environmental compliance. ECOPACK[®] specifications, grade definitions and product status are available at: www.st.com. ECOPACK[®] is an ST trademark.

Table 10. VFQFPN8 (4x4x1.08 mm) mechanical data

| Dim. | mm | | |
|------|------|------|------|
| | Min. | Typ. | Max. |
| A | 0.80 | 0.90 | 1.00 |
| A1 | | 0.02 | 0.05 |
| A3 | | 0.20 | |
| b | 0.23 | 0.30 | 0.38 |
| D | 3.90 | 4.00 | 4.10 |
| D2 | 2.82 | 3.00 | 3.23 |
| E | 3.90 | 4.00 | 4.10 |
| E2 | 2.05 | 2.20 | 2.30 |
| e | | 0.80 | |
| L | 0.40 | 0.50 | 0.60 |

Figure 32. VFQFPN8 (4x4x1.08 mm) package dimensions

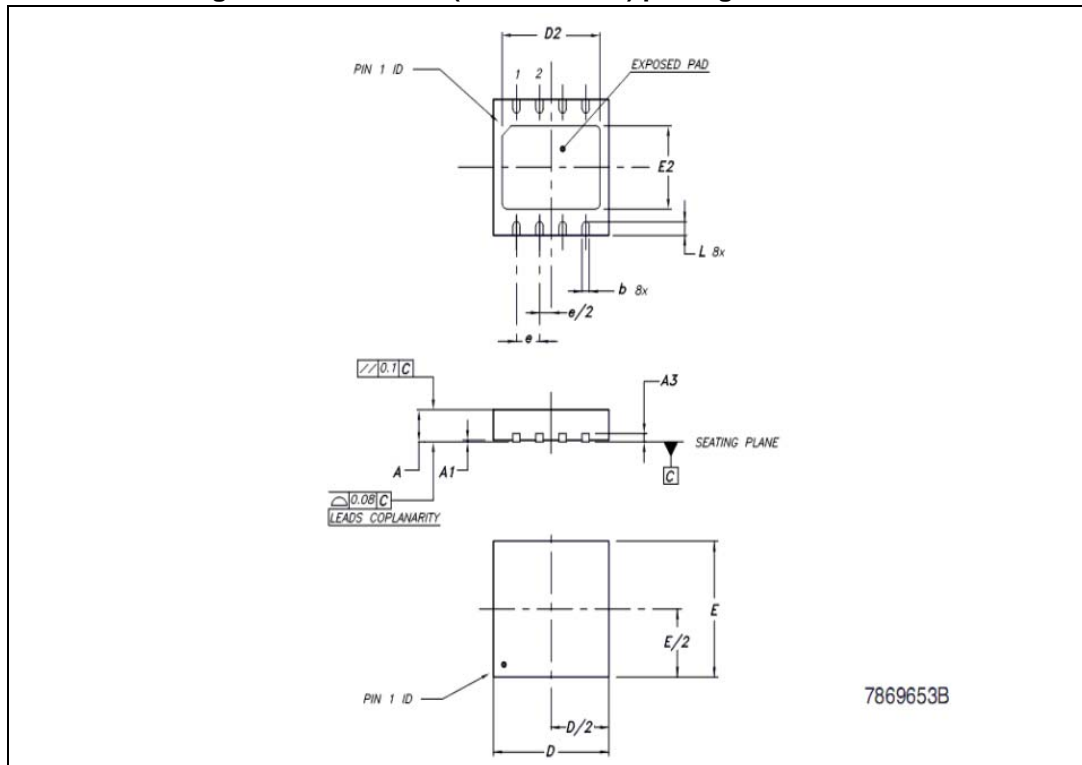
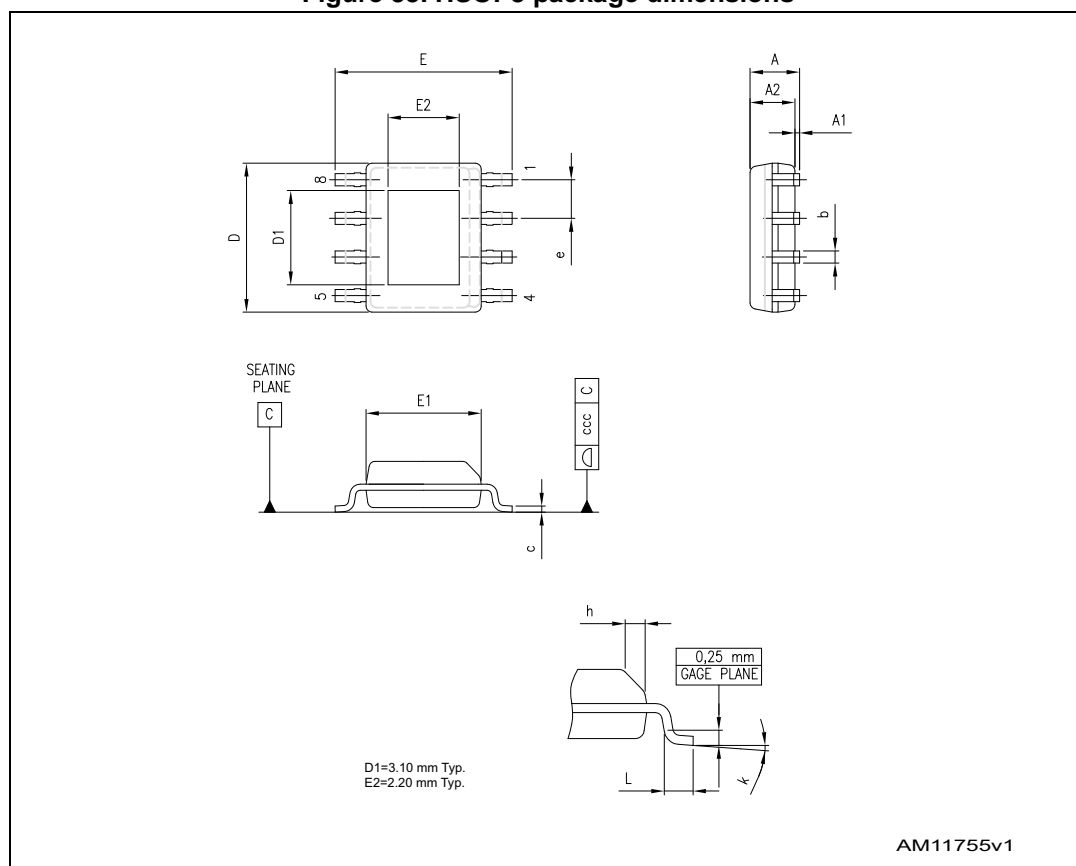


Table 11. HSOP8 mechanical data

| Dim | mm | | |
|-----|------|------|-------|
| | Min. | Typ. | Max. |
| A | | | 1.70 |
| A1 | 0.00 | | 0.150 |
| A2 | 1.25 | | |
| b | 0.31 | | 0.51 |
| c | 0.17 | | 0.25 |
| D | 4.80 | 4.90 | 5.00 |
| E | 5.80 | 6.00 | 6.20 |
| E1 | 3.80 | 3.90 | 4.00 |
| e | | 1.27 | |
| h | 0.25 | | 0.50 |
| L | 0.40 | | 1.27 |
| k | 0.00 | | 8.00 |
| ccc | | | 0.10 |

Figure 33. HSOP8 package dimensions



11 Revision history

Table 12. Document revision history

| Date | Revision | Changes |
|-------------|----------|------------------|
| 20-May-2013 | 1 | Initial release. |

Please Read Carefully:

Information in this document is provided solely in connection with ST products. STMicroelectronics NV and its subsidiaries ("ST") reserve the right to make changes, corrections, modifications or improvements, to this document, and the products and services described herein at any time, without notice.

All ST products are sold pursuant to ST's terms and conditions of sale.

Purchasers are solely responsible for the choice, selection and use of the ST products and services described herein, and ST assumes no liability whatsoever relating to the choice, selection or use of the ST products and services described herein.

No license, express or implied, by estoppel or otherwise, to any intellectual property rights is granted under this document. If any part of this document refers to any third party products or services it shall not be deemed a license grant by ST for the use of such third party products or services, or any intellectual property contained therein or considered as a warranty covering the use in any manner whatsoever of such third party products or services or any intellectual property contained therein.

UNLESS OTHERWISE SET FORTH IN ST'S TERMS AND CONDITIONS OF SALE ST DISCLAIMS ANY EXPRESS OR IMPLIED WARRANTY WITH RESPECT TO THE USE AND/OR SALE OF ST PRODUCTS INCLUDING WITHOUT LIMITATION IMPLIED WARRANTIES OF MERCHANTABILITY, FITNESS FOR A PARTICULAR PURPOSE (AND THEIR EQUIVALENTS UNDER THE LAWS OF ANY JURISDICTION), OR INFRINGEMENT OF ANY PATENT, COPYRIGHT OR OTHER INTELLECTUAL PROPERTY RIGHT.

ST PRODUCTS ARE NOT AUTHORIZED FOR USE IN WEAPONS. NOR ARE ST PRODUCTS DESIGNED OR AUTHORIZED FOR USE IN: (A) SAFETY CRITICAL APPLICATIONS SUCH AS LIFE SUPPORTING, ACTIVE IMPLANTED DEVICES OR SYSTEMS WITH PRODUCT FUNCTIONAL SAFETY REQUIREMENTS; (B) AERONAUTIC APPLICATIONS; (C) AUTOMOTIVE APPLICATIONS OR ENVIRONMENTS, AND/OR (D) AEROSPACE APPLICATIONS OR ENVIRONMENTS. WHERE ST PRODUCTS ARE NOT DESIGNED FOR SUCH USE, THE PURCHASER SHALL USE PRODUCTS AT PURCHASER'S SOLE RISK, EVEN IF ST HAS BEEN INFORMED IN WRITING OF SUCH USAGE, UNLESS A PRODUCT IS EXPRESSLY DESIGNATED BY ST AS BEING INTENDED FOR "AUTOMOTIVE, AUTOMOTIVE SAFETY OR MEDICAL" INDUSTRY DOMAINS ACCORDING TO ST PRODUCT DESIGN SPECIFICATIONS. PRODUCTS FORMALLY ESCC, QML OR JAN QUALIFIED ARE DEEMED SUITABLE FOR USE IN AEROSPACE BY THE CORRESPONDING GOVERNMENTAL AGENCY.

Resale of ST products with provisions different from the statements and/or technical features set forth in this document shall immediately void any warranty granted by ST for the ST product or service described herein and shall not create or extend in any manner whatsoever, any liability of ST.

ST and the ST logo are trademarks or registered trademarks of ST in various countries.

Information in this document supersedes and replaces all information previously supplied.

The ST logo is a registered trademark of STMicroelectronics. All other names are the property of their respective owners.

© 2013 STMicroelectronics - All rights reserved

STMicroelectronics group of companies

Australia - Belgium - Brazil - Canada - China - Czech Republic - Finland - France - Germany - Hong Kong - India - Israel - Italy - Japan - Malaysia - Malta - Morocco - Philippines - Singapore - Spain - Sweden - Switzerland - United Kingdom - United States of America

www.st.com